URSI GASS 2021, Rome, Italy, 28 August - 4 September 2021

D-Band Radiating Near field Channel Impulse Response Characterization using Time Delay Profile

Priyansha Kaurav(1), Shiban Koul (1), and Ananjan Basu(1)
(1) CARE, IIT Delhi, Hauz Khas, Delhi http://www.care.iitd.ac.in

Abstract

In this paper, we present characterization and measurement of a D-band (110-170 GHz) radiating near field channel. Assuming 2-ray path model, Channel Impulse Response (C.I.R) has been theoretically improvised for a bandlimited frequency response obtained from V.N.A. The change in CIR with increase in radiating near field distance between the transmitter and receiver has been studied using time delay statistical parameter i.e. root mean square (RMS) delay spread variation with distance. Furthermore, the effect of change in height of transmitter and receiver on RMS delay has been analyzed theoretically and experimentally validated using near field measurement setup. The experiment has been conducted using D- band 16dBi horn antennas working as the transmitter and receiver.

1 Introduction

With the onset of 5G technology, the communication industry has been involved in extensive research work in 28 GHz, 38 GHz, 60 GHz and 73 GHz frequency bands [1]. As the demand for high-speed wireless communication is growing, interest is being shifted to higher frequency ranges that can provide large bandwidth along with high data rates [1-4].

D-band which is 110-170 GHz frequency band offers a large bandwidth of 60 GHz, has been recently explored for various applications in wireless short-range communications, velocity sensor, on-body health monitoring systems [5],[6]. Since this band provides a spatial resolution of 5mm, it can also be explored in imaging applications for biomedical applications the advantage over x-ray being the non-ionizing nature of millimeter wave [7]. While D band far field propagation mechanism has been demonstrated by [1],[2],[8] and others, to the best of our knowledge no *near field D band characterization* has been reported in the open literature.

As the first step towards characterizing the radiating near field D band channel, we first used the classical 2R model [9], which is the superposition of Line of Sight (LOS) ray and ray reflected from the ground for characterizing the channel. The contribution of this paper is as follows:

1) Optimization of the Channel Impulse Response (CIR) function for bandlimited frequency response, the reason being the bandlimited nature of acquired transmission parameters from VNA.
2) Study of the change in CIR characteristics with the change in distance between the transmitter and receiver in radiating near field zone using RMS delay spread profile.
3) Effect of change in height of transmitter and receiver on CIR by analyzing the RMS delay spread change. The theoretical results are verified using an experimental setup consisting of two similar D-band horn antennas of 16 dBi gain working as transmitter and receiver.

The rest of the paper is organized as follows. Section 2 describes the measurement setup and measurement scenario for conducting the experiment. Section 3 presents the theoretical analysis followed by the measurement results and Section 4 gives the concluding remarks of the paper.

2 Measurement

2.1 Measurement Setup

The D-band measurement setup consists of VNA(Keysight Technologies N5247B) with a pair of frequency extenders from Virginia Diodes, Inc. working in the range of 110-170 GHz. For all the measurements, test signal power of 9dBm is utilized providing a typical dynamic range of 120 dB for intermediate frequency bandwidth of 100 Hz. For 60 GHz bandwidth range of measurement, 801 sweep points are taken, giving the maximum excess delay of 13ns. All the equipment characteristics are summarized in table 1. The block diagram of measurement setup including transmitter and receiver is shown in Fig. 1.

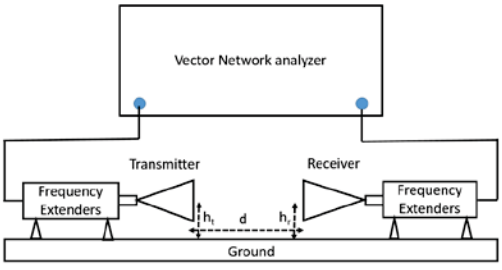

Figure 1. Block Diagram of Measurement Setup

Table 1. Measurement Equipment Characteristics

Parameter	Symbol	Value
Start Frequency	f_{start}	110 GHz
Stop Frequency	f_{stop}	170 GHz
Bandwidth	B	60 GHz
Sweep Points	N	801
Excess Delay	τ_{excess}	13ns
Input power	P_{in}	9dBm

2.2 Antenna Characteristics

Two similar pyramidal horn antennas with gain varying from 14dB to 17 dB from 110 GHz to 170 GHz are used as transmitter and receiver as shown in Fig.2. The measured S_{11} and frequency dependent gain are presented in Fig.3. The return loss is below 20 dB for all the frequency range. [10] gives the radiating near field range of antenna as:

$$0.62 * \sqrt{\frac{l^3}{\lambda}} < r < \frac{2*l^2}{\lambda} \quad (1)$$

Where, l is the sum of diagonal lengths of the transmitter and receiver antenna. In our case, 3cm to 14cm is the radiating near field range.

Figure 2. Pyramidal horn antennas as transmitter and receiver

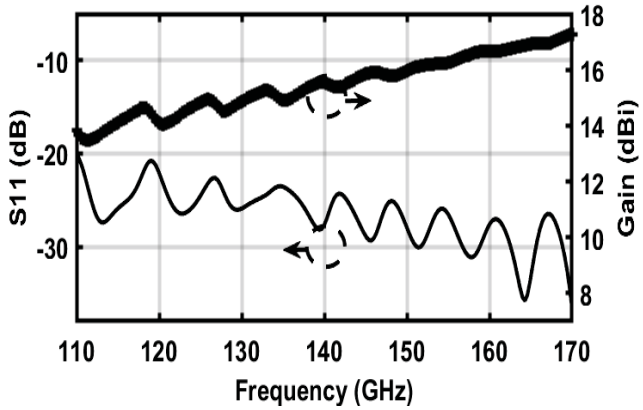

Figure 3. Return Loss and Gain of horn antenna

2.3 Measurement Scenario

The measurement campaign is conducted for LoS case where the separation distance between the transmitter and receiver antenna is varied from 3cm to 16cm in the step of 0.5cm giving a total of 27 sets of transmission parameters (S_{21}). The measurement covers the range from radiating near field to far field scenario. During our measurements, the location of the Tx is fixed, Rx is moved away from the Tx antenna for the predefined separations.

To study the impact of ground reflections in channel impulse response height of both Tx and Rx is varied from 4cm to 6cm in the step of 0.5cm. Fig. 4 shows the measurement setup including the absorbers around the antennas to mitigate the reflections and side lobe effects. All the analysis is done taking transmitter and receiver antenna as a part of the channel impulse response.

Figure 4: Radiating near field measurement setup

3 Analysis and Results

3.1 Channel Impulse Response

In 2-ray reflection model, the channel impulse response (CIR), h (τ) is given by (2) from [9]:

$$h(\tau) \approx \frac{\lambda\sqrt{G^t G^r}}{4\pi d}(\delta(\tau) - \delta(\tau - \frac{2h_t h_r}{d}\frac{1}{c})) \quad (2)$$

where, G^t and G^r are the gain of transmitter and receiver antenna, h_t and h_r are the height of transmitter and receiver respectively, d is the separation between the transmitter and receiver. We assume that the path length difference between the direct ray and ground reflected ray, $\Delta l \approx \frac{2h_t h_r}{d}$ as used in [2].

To determine the channel impulse response using experimental setup, IDFT is taken for the measured frequency response. In order to keep in account the band limited nature of S_{21} parameters obtained from VNA, we

convolve the delta ($\delta(.)$) function with the sinc(.) function modifying (2) as (3):

$$h(\tau) \approx \frac{\lambda\sqrt{G^t G^r}}{4\pi d}(sinc(\tau) - sinc(\tau - \frac{2h_t h_r}{d}\frac{1}{c})) \qquad (3)$$

3.2 Power Delay Profile and RMS Delay

Statistical characterization is done to study the impact of separation between transmitter and receiver (d) in radiating near field region on the CIR function obtained in (3). Mean excess delay spread and root mean square (RMS) delay spread represent the statistical parameters of CIR [3,4].

Following steps are performed in MATLAB in order to evaluate the relation between RMS delay spread of CIR and the separation between transmitter and receiver (d):

Step 1: The Power Delay Profile (PDP) curve is plotted using the normalized squared amplitude response of CIR ($|h(t-t_0)|^2$) . t_0 represents the time origin which is chosen as the time instant where the power intensity is maximum as shown in Fig. 5.

Step 2: Using the PDP curve, mean excess delay τ_m [11] is calculated which is given as (4):

$$\tau_m = \frac{\int t*|h(t-t_0,d)|^2 dt}{\int |h(t-t_0,d)|^2 dt} \qquad (4)$$

Step 3: Finally Root mean square delay spread τ_{rms} [11] is obtained from Power Delay Profile curve which estimates the spread around the maximum intensity profile. It is given by (5):

$$\tau_{rms} = \sqrt{\frac{\int (t-\tau_m)^2 * |h(t-t_0,d)|^2 dt}{\int |h(t-t_0,d)|^2 dt}} \qquad (5)$$

Using the above steps τ_{rms} is evaluated for various separations from 3cm to 16cm. It is observed from RMS delay versus the separation curve that τ_{rms} increases with d as shown in Fig.6. This can be explained from (3) as d increases the separation between the two sinc functions of direct path and reflected path tends to decrease leading to decrease in τ_m thereby increase in τ_{rms}.

To study the impact of change in height of the transmitter and receiver in RMS delay spread in the radiating near field region, step 1 to 3 are followed for heights of transmitter and receiver from 4cm to 6cm in the steps of 5mm. Fig. 6 shows the τ_{rms} versus d curve for all the heights. It is observed that τ_{rms} decreases with increase in height, the reason being increase in distance between two sinc pulses in CIR function in (3), leading to increase in τ_m which in turn decreases τ_{rms}.

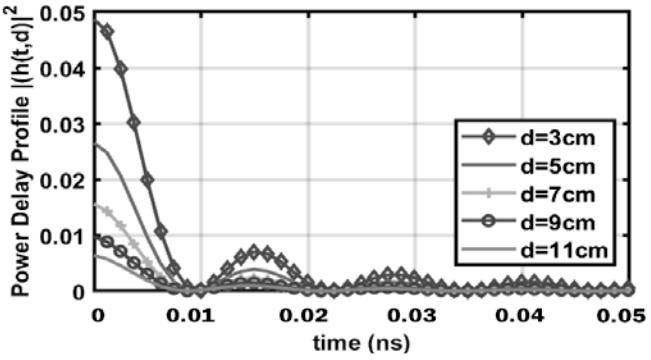

Figure 5. Power Delay Profile plots for various separations of near field separations

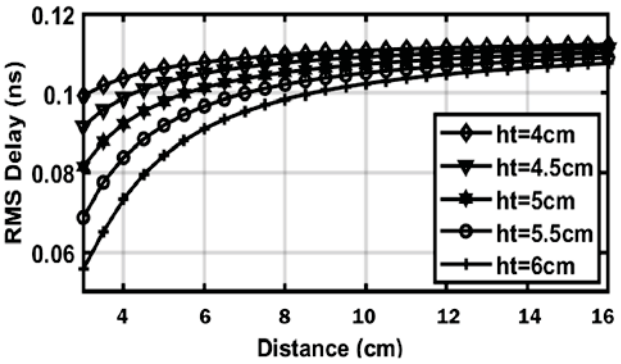

Figure 6. RMS Delay spread versus distance plot for different heights of transmitter and receiver

3.3 Measurement Results

To verify the CIR function obtained in (3), an experimental procedure is performed using the measurement setup described in Section 2. The S_{21} parameters are acquired from VNA in 110-170 GHz frequency range for separations 3cm to 14 cm in the step of 0.5cm for each height parameter of the transmitter and receiver ranging from 4cm to 6cm. The acquired parameters are then converted into time domain using IDFT in MATLAB providing measured time domain Channel Impulse Response . The obtained CIRs for all the parameters are then used to plot τ_{rms} versus separation curve for various heights using steps 1 to 3 from section 3.2. Fig 7 shows the PDP versus time curve for various separations using the experimental data. We observe that PDP of the measured response resembles the PDP obtained from the simulated CIR response in Fig 5.

Fig. 8 shows the τ_{rms} versus d curve for all the heights. τ_{rms} shows an incremental variation with increase in separation between transmitter and receiver, while the value decreases for increase in height for a particular separation distance d similar to the simulated τ_{rms} in Fig. 6. Thus, we observe that (3) can be used to model CIR in radiating near field region in millimeter band provided there are no other reflections from the surrounding regions and side lobe level effects are mitigated.

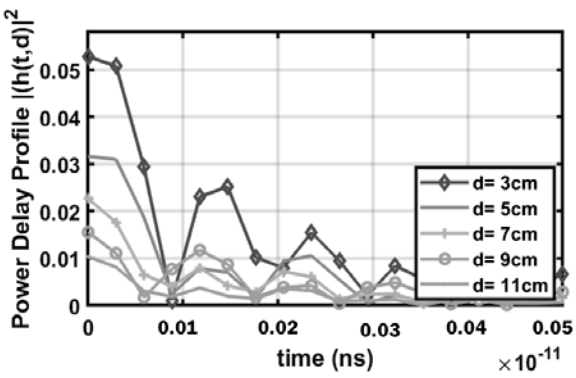

Figure 7. Power Delay profile plot for various separations between transmitter and receiver using experimental setup

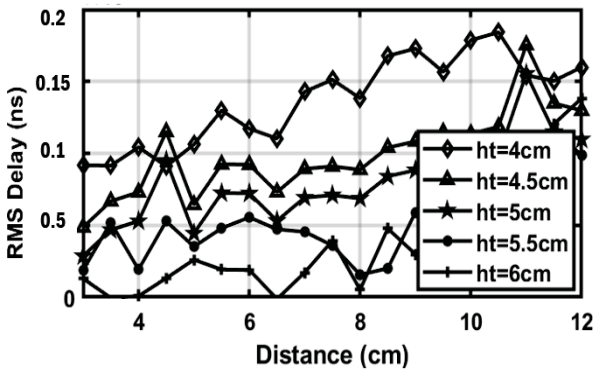

Figure 8. RMS delay spread versus distance curve for various heights using experimental setup

4 Conclusion

This paper presents the theoretical analysis of channel impulse response of the radiating near field D-band channel. The channel impulse response function is optimized for the acquired bandlimited nature of transmission parameters measured from the VNA. Time delay profile analysis is performed to study the effect of increase in separation and height of the transmitter and receiver on channel impulse response function. It is observed that the RMS delay spread function of the CIR increases with increase in separation and decreases with increase in height due to the change in overlap of 2 sinc pulses of LOS and ground reflected ray. Finally, the theoretical analysis is validated by the measurement results where two pyramidal horn antennas are used as the transmitter and receiver.

5 Acknowledgment

The authors wish to acknowledge the support of the IIT Delhi and Defence Research and Development Organization (DRDO) for establishment of VNA measurement facility in Centre of Applied Research in electronics (CARE) Dept. that can measure up to 1.1 THz

6 References

[1] Y. Xing and T. S. Rappaport, "Propagation Measurement System and Approach at 140 GHz-Moving to 6G and Above 100 GHz," 2018 IEEE Global Communications Conference (GLOBECOM), Abu Dhabi, United Arab Emirates, 2018, pp. 1-6.

[2] S. Kim, W. T. Khan, A. Zajić, J. Papapolymerou, "D-band channel measurements and characterization for indoor applications", IEEE Trans. Antennas Propag., vol. 63, no. 7, pp. 3198-3207, Jul. 2015.

[3] T. Kosugi et al., "120-GHz Tx/Rx waveuide modules for 10-Gbit/s wireless link system," in Proc. IEEE CSICS Dig., Oct. 2006, pp. 25–28.

[4] S. Priebe et al., "A comparison of indoor channel measurements and ray tracing simulations at 300 GHz," in Proc. Int. Conf. Infrared Millim. Terahertz Waves (IRMMW-THz), Sep. 5–10, 2010, pp. 1–2.

[5] O. Kanhere and T. S. Rappaport, "Position locationing for millimeter wave systems," in IEEE 2018 Global Communications Conference, Dec.2018, pp. 1–6.

[6] T. S. Rappaport, J. N. Murdock, and F. Gutierrez, "State of the art in 60-GHz integrated circuits and systems for wireless communications," Proceedings of the IEEE, vol. 99, no. 8, pp. 1390–1436, Aug. 2011.

[7] E. Aguilar, A. Hagelauer, D. Kissinger and R. Weigel, "A low-power wideband D-band LNA in a 130 nm BiCMOS technology for imaging applications," 2018 IEEE 18th Topical Meeting on Silicon Monolithic Integrated Circuits in RF Systems (SiRF), Anaheim, CA, 2018, pp. 27-29.

[8] G. R. MacCartney and T. S. Rappaport, "A flexible millimeter-wave channel sounder with absolute timing," IEEE Journal on Selected Areas in Communications, vol. 35, no. 6, pp. 1402–1418, June 2017.

[9] E. Zöchmann, K. Guan and M. Rupp, "Two-ray models in mmWave communications," *2017 IEEE 18th International Workshop on Signal Processing Advances in Wireless Communications (SPAWC)*, Sapporo, pp. 1-5,2017.

[10] C. Balanis, Antenna Theory, Wiley, 1997.

[11] A. F. Molisch, *Wireless Communications*. Wiley Publishing, 2nd ed., 2011.

[12] C. L. Holloway, M. G. Cotton and P. McKenna, "A model for predicting the power delay profile characteristics inside a room." *IEEE Transactions on Vehicular Technology*, vol. 48, no. 4, pp. 1110-1120, July 1999.